Journal of General Virology (2008), **89**, 2080–2089 **DOI** 10.1099/vir.0.2008/001404-0

Glucose-6-phosphate dehydrogenase deficiency enhances enterovirus 71 infection

Hung-Yao Ho,[1]† Mei-Ling Cheng,[1,2]† Shiue-Fen Weng,[1] Lo Chang,[1] Tsun-Tsun Yeh,[1] Shin-Ru Shih[1,3,4] and Daniel Tsun-Yee Chiu[1,3,4]

Correspondence
Daniel Tsun-Yee Chiu
dtychiu@mail.cgu.edu.tw

Shin-Ru Shih
srshih@mail.cgu.edu.tw

[1]Graduate Institute of Medical Biotechnology and Department of Medical Biotechnology and Laboratory Science, Chang Gung University, Kwei-san, Tao-yuan, Taiwan, ROC

[2]Center for Gerontological Research, Chang Gung University, Kwei-san, Tao-yuan, Taiwan, ROC

[3]Graduate Institute of Basic Medical Sciences, Chang Gung University, Kwei-san, Tao-yuan, Taiwan, ROC

[4]Department of Clinical Pathology, Chang Gung Memorial Hospital, Kwei-san, Tao-yuan, Taiwan, ROC

Variations in the cellular microenvironment affect the host's susceptibility to pathogens. Using glucose-6-phosphate dehydrogenase (G6PD)-deficient fibroblasts as a model, this study demonstrated that the cellular redox status affects infectivity as well as the outcome of enterovirus 71 (EV71) infection. Compared with their normal counterparts, G6PD-deficient cells supported EV71 replication more efficiently and showed greater cytopathic effect and loss of viability. Mechanistically, viral infection led to increased oxidative stress, as indicated by increased dichlorofluorescein fluorescence and a diminished ratio of glutathione (GSH) to its disulfide form (GSSG), with the effect being greater in G6PD-deficient cells. Exogenous expression of active G6PD in the deficient cells, which increased the intracellular GSH : GSSG ratio, suppressed the generation of viral progeny. Consistent with this, treatment with *N*-acetylcysteine offered resistance to EV71 propagation and a cytoprotective effect on the infected cells. These findings support the notion that G6PD status, and thus redox balance, is an important determinant of enteroviral infection.

Received 18 February 2008
Accepted 16 May 2008

INTRODUCTION

Glucose-6-phosphate dehydrogenase (G6PD) has recently been implicated in the regulation of cell growth and survival, replicative senescence and development (Ho *et al.*, 2005, 2007b). We recently found that G6PD-deficient cells undergo premature senescence upon serial passage and show an increased propensity for oxidant-induced senescence (Beck *et al.*, 2001; Cheng *et al.*, 2004; Ho *et al.*, 2000, 2007a). In addition, these cells are more susceptible to oxidant-induced apoptosis (Ho *et al.*, 2006) and display altered growth responses to signalling factor (Cheng *et al.*, 2000). Such diverse effects are probably attributable to the biochemical role of G6PD as a major source of reducing equivalents. Clinically, G6PD deficiency, affecting over 200 million individuals worldwide, can cause neonatal jaundice, drug- or infection-induced haemolytic crisis, favism and, less commonly, non-spherocytic haemolytic anaemia (Beutler, 1991; Luzzatto & Battistuzzi, 1985). Moreover, it is associated with poor prognosis in patients with nasopharyngeal carcinoma (Cheng *et al.*, 2001) and with increased risk for diabetes mellitus (Wan *et al.*, 2002). Given its important physiological role in nucleated cells, G6PD deficiency may cause more health problems than previously thought. G6PD-deficient cells provide a cellular system for studying the relationship between oxidative stress and such human disease as viral infection.

Enterovirus 71 (EV71) is a non-enveloped RNA virus within the family *Picornaviridae* (Racaniello, 2001). Since the initial identification of EV71 in California in 1969 (Schmidt *et al.*, 1974), outbreaks of EV71 infection have been recognized periodically throughout the world (Ho *et al.*, 1999; Lin *et al.*, 2002; Liu *et al.*, 2000; McMinn, 2002). The clinical manifestation of EV71 infection may include febrile illness, acute respiratory disease, hand-foot-and-mouth disease, herpangina, myocarditis, aseptic meningitis, acute flaccid paralysis, brainstem and/or cerebellar encephalitis, Guillain–Barré syndrome or combinations of these clinical features (Ishimaru *et al.*, 1980; McMinn, 2002; Takimoto *et al.*, 1998). Children under 5 years of age are especially susceptible to these syndromes and may develop permanent neurological sequelae or even succumb to such disorders (Huang *et al.*, 1999). The largest epidemic of EV71 to date occurred in Taiwan in 1998:

†These authors contributed equally to this paper.

nearly 130 000 cases, of which 405 cases were severe, were reported over a period of 8 months (Ho *et al.*, 1999; Lin *et al.*, 2002). Since then, EV71 infection has recurred every year in Taiwan and continues to circulate in the Asia–Pacific region (Lin *et al.*, 2003; McMinn, 2002).

There is accumulating evidence that oxidative stress affects the interactions between host and viral pathogens, and hence viral pathogenesis. Susceptibility to infection with coxsackievirus and influenza virus is modulated by the redox environment (Beck *et al.*, 2000, 2003a; Cai *et al.*, 2003). *In vivo* studies have demonstrated that coxsackievirus replicates to a higher titre in C3H/HeJ mice fed a high-iron diet or deficient in selenium and/or vitamin E (Beck *et al.*, 1994a, b, 2000, 2005). Another mouse strain, C57BL/6, which is normally resistant to coxsackievirus B3-induced myocarditis, became susceptible when fed a selenium- and vitamin E-deficient diet (Beck *et al.*, 2003b). It is speculative whether the redox status affects the replication and pathogenicity of other viruses. Investigations into the relationship between the host's redox status and virus virulence are of great value in developing therapeutic strategies against clinically relevant viruses such as EV71.

In the present study, we demonstrated that the infectivity and virulence of EV71 are enhanced in G6PD-deficient cells. EV71 infection caused oxidative stress, with the effect being significantly greater in G6PD-deficient cells than in their normal counterparts. Exogenous expression of G6PD and *N*-acetylcysteine treatment suppressed the generation of progeny infectious virions and conferred a protective effect on the infected cells. Our findings suggest that G6PD status, and hence the redox status, modulates the infectivity of EV71 and the outcome of infection.

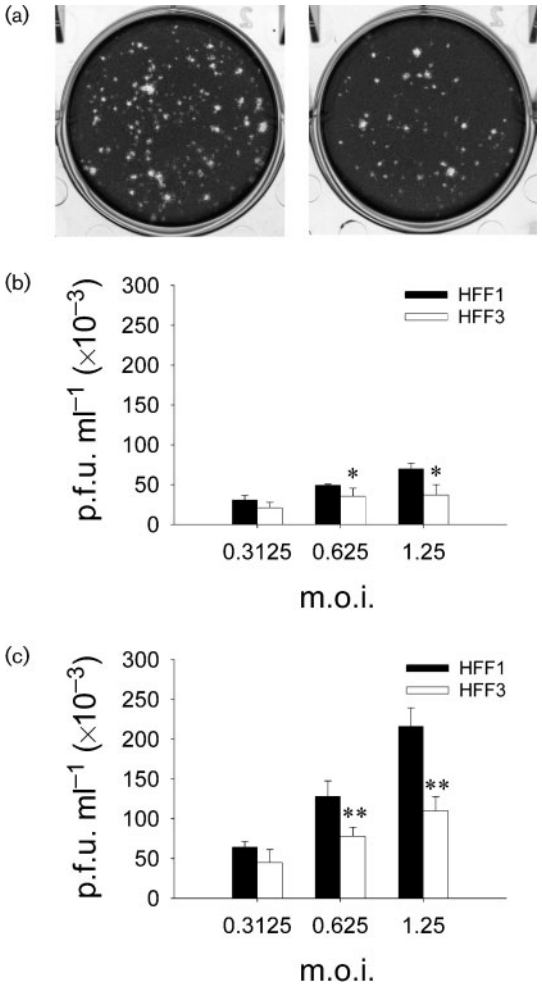

Fig. 1. Increased production of infectious viral particles in G6PD-deficient cells. (a) A typical plaque assay result showing that HFF1 cells (left panel) produce more infectious particles than HFF3 cells (right panel) at 24 h p.i. at an m.o.i. of 1.25. (b, c) HFF1 and HFF3 cells were infected with EV71 at the indicated m.o.i. Progeny viral particles were quantified at 24 (b) or 48 (c) h p.i. Data are expressed as p.f.u. (ml lysate)$^{-1}$. The results are presented as means ± SD of six separate experiments. *, $P<0.05$ and **, $P<0.01$ (HFF3 vs HFF1).

METHODS

Cell culture and propagation of EV71. Primary human foreskin fibroblasts (HFF3) and their G6PD-deficient counterparts (HFF1) were isolated as described previously (Cheng *et al.*, 2004; Ho *et al.*, 2000). HFF1 cells were derived from the foreskin of a neonate carrying the Taiwan Hakka (G6PD^{1376T}) variant of the G6PD gene. Cells were cultured in Dulbecco's modified Eagle's medium (DMEM) supplemented with 10 % fetal calf serum (FCS), 100 U penicillin ml^{-1}, 0.1 mg streptomycin ml^{-1} and 0.25 μg amphotericin ml^{-1} at 37 °C in a humidified atmosphere of 5 % CO_2. Cells at a population doubling level of 15–20 were used in experiments throughout the study. Vero cells (ATCC CCL-81) were cultured in modified Eagle's medium (MEM) supplemented with 10 % FCS, 100 U penicillin ml^{-1}, 0.1 mg streptomycin ml^{-1} and 0.25 μg amphotericin ml^{-1} in an atmosphere of 5 % CO_2 at 37 °C. Cell lines LGIN and LKGIN, which exogenously express G6PD, and a control cell line expressing green fluorescent protein, LEIN, were derived from HFF1 cells as described elsewhere (Cheng *et al.*, 2004; Ho *et al.*, 2000).

EV71 (BrCr strain; ATCC VR784) was propagated in Vero cells as described previously with modifications (Shih *et al.*, 2004). After the culture reached 80 % confluency in a T150 flask, the cells were washed twice with PBS and incubated with viral inoculum at 37 °C for 1 h. The flask was gently agitated at 20 min intervals during the adsorption period. The viral inoculum was then removed and fresh medium containing 1 % FCS and antibiotics was added. Cells were incubated in a humidified atmosphere of 5 % CO_2 at 37 °C. When >90 % cytopathic effect (CPE) was visible in the culture, the viral supernatant was collected and cell debris removed by centrifugation. Any remaining viral particles were released from the cell debris by three successive freeze–thaw cycles and subsequent centrifugation. Finally, all supernatants were pooled and stored at −80 °C. This procedure was also used to quantify progeny virus production in HFF1 and HFF3 cells, with the exception that 1×10^4 cells were seeded in each well of a 24-well culture plate and the progeny virions were harvested in 1 ml DMEM/1 % FCS.

Plaque assay. Vero cells (3.8×10^5 cells per well) were seeded into a six-well culture plate, incubated overnight and then infected with a

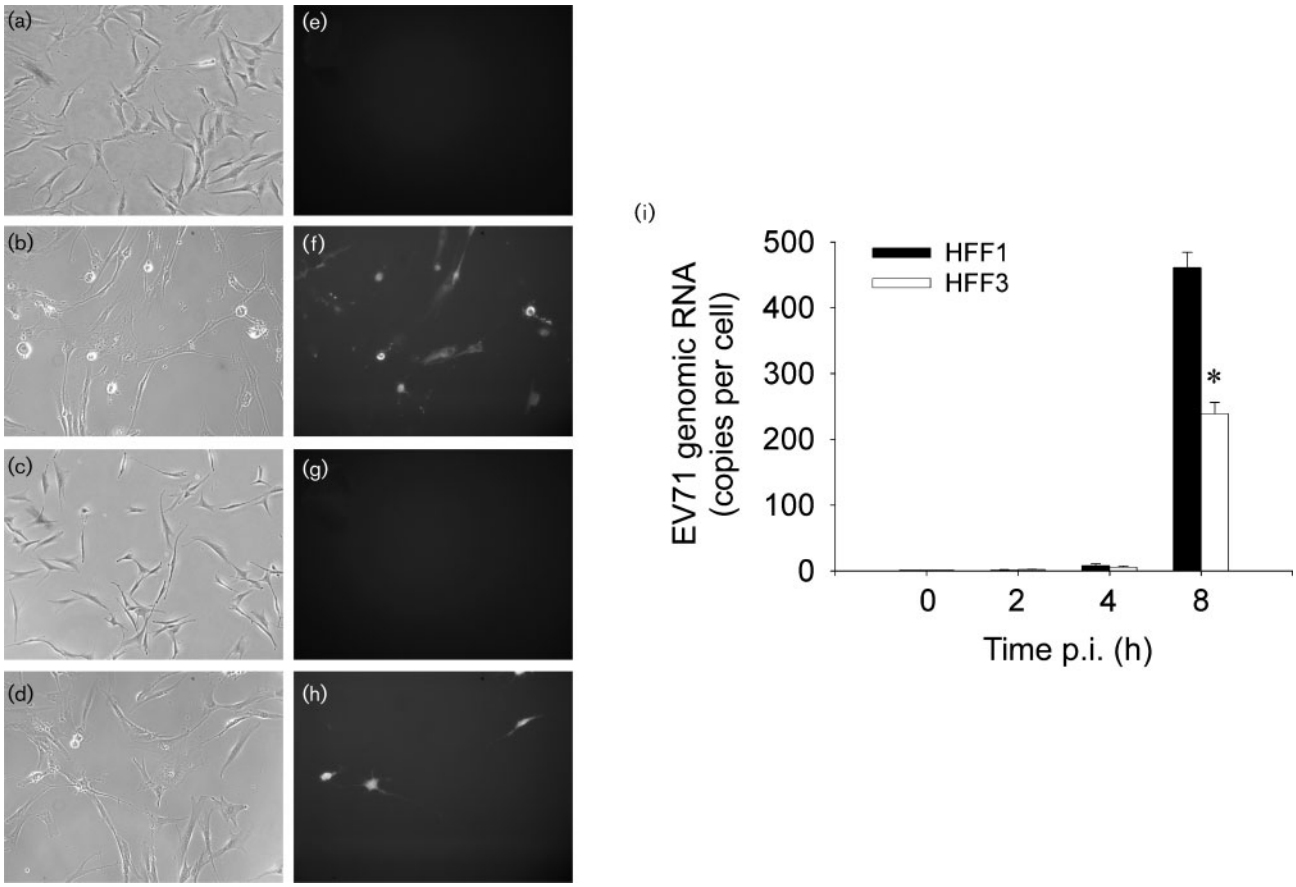

Fig. 2. G6PD deficiency enhances EV71 replication. (a–h) HFF1 (a, b, e, f) and HFF3 (c, d, g, h) cells were left uninfected (a, c, e, g) or were infected (b, d, f, h) with EV71 at an m.o.i. of 1.25. Infected cells were examined under a fluorescence microscope for viral protein expression (e–h). The corresponding phase-contrast micrographs (a–d) are also shown. The results shown are representative of three experiments. Original magnification ×200. (i) HFF1 and HFF3 cells were infected with EV71 at an m.o.i. of 1.25. At the indicated times p.i., levels of EV71 genomic RNA were quantified by PCR. The results are presented as means ± SD of six separate experiments. *, $P<0.01$ (HFF3 vs HFF1).

10-fold serially diluted virus suspension. After 60 min adsorption, the cells were washed once with PBS and overlaid with 0.3 % agarose in MEM/2 % FCS. After 96 h, the cells were fixed with 10 % formaldehyde and then stained with 1 % crystal violet solution. The virus titre was quantified as p.f.u. (ml cell lysate^{-1}).

Detection of EV71 viral protein. To detect expression of EV71 viral protein in infected cells, 2×10^4 cells were seeded into a 12-well glass-bottomed culture plate and 24 h later were infected with virus at an m.o.i. of 1.25. At 48 h post-infection (p.i.), the cells were washed once with PBS and fixed with 3.7 % formaldehyde at room temperature for 5 min. The fixed cells were rinsed three times with PBS containing 0.05 % Tween 20 (PBST) and blocked with 1 % BSA/PBST at 37 °C for 15 min. Cells were then incubated with anti-EV71 monoclonal antibody (Chemicon) at 37 °C for 60 min, rinsed with PBST and incubated with FITC-conjugated anti-mouse IgG (Chemicon) for 30 min. After several rinses in PBST, the cells were examined under a fluorescence microscope.

Quantitative PCR analysis of EV71. Virus was allowed to adsorb to HFF1 or HFF3 cells for 1 h. Total RNA was extracted from infected cells using a Viral RNA Extraction Miniprep kit (Viogene) according to the manufacturer's instruction. Total RNA (1 μg) was reverse-transcribed into cDNA using a SuperScript First-Strand Synthesis kit (Invitrogen). One microlitre of a 1 : 100 dilution of the cDNA reaction was amplified using forward and reverse primers for the EV71 genome and β-actin as a control, using a SYBR Green PCR Master Mix (Applied Biosystems). The forward and reverse EV71 primers were 5′-ACTGACCAAGGACACTTCAC-3′ and 5′-CCAGTGTGAGTTCCAAGTTT-3′, respectively. The forward and reverse β-actin primers were 5′-ATCGTGCGTGACATTAAGGAG-3′ and 5′-CCATCTCTTGCTCGAAGTCC-3′, respectively. The reactions were performed in a GeneAmp 5700 sequence detection system (Applied Biosystems) under the following thermal cycling conditions: 94 °C for 10 min, followed by 40 cycles of 94 °C for 30 s, 55 °C for 30 s and 72 °C for 60 s. The threshold cycle value was normalized to that of β-actin.

Determination of cell viability. Cell viability was determined using a 3-(4,5-dimethylthiazol-2-yl)-2,5-diphenyltetrazolium bromide (MTT) assay (Denizot & Lang, 1986). Briefly, cells were incubated with 0.5 mg MTT ml^{-1} at 37 °C for 2 h. After removal of culture

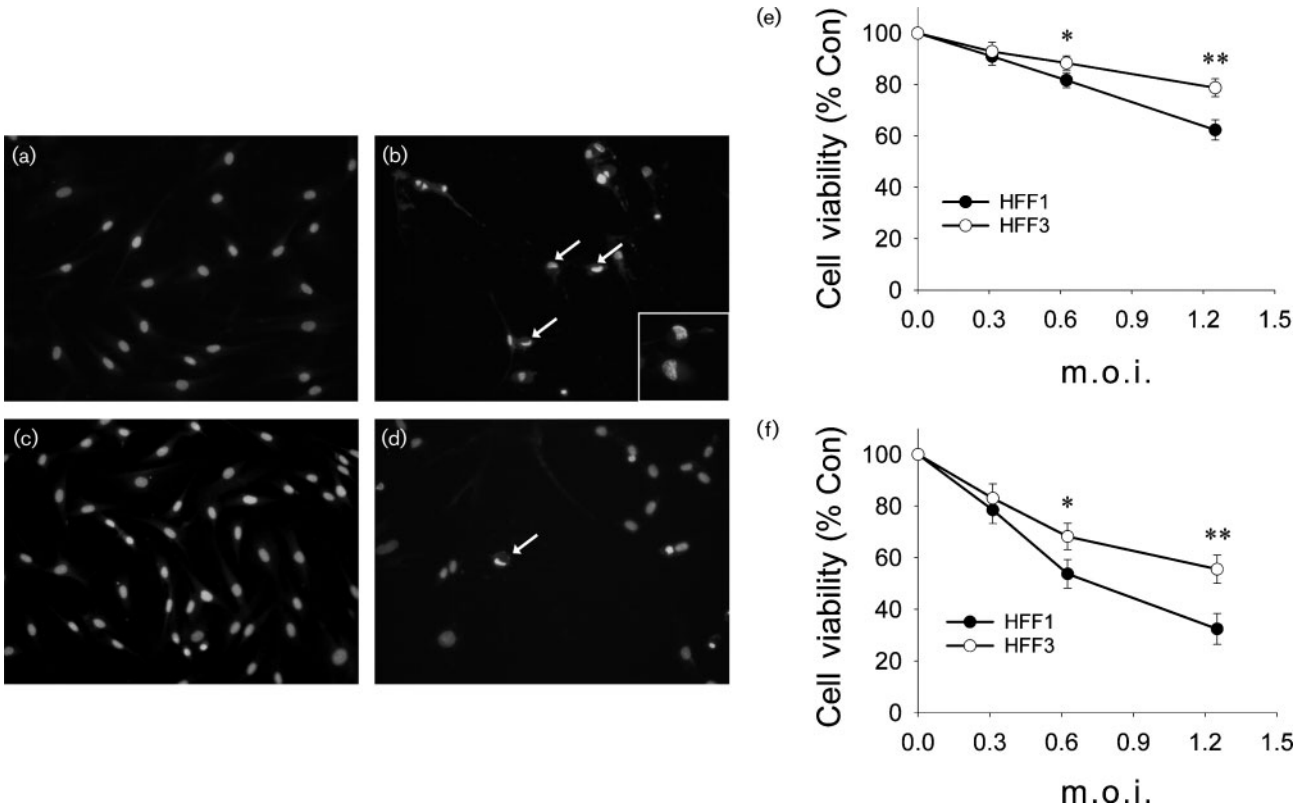

Fig. 3. Enhanced CPE of EV71 in G6PD-deficient cells. (a–d) HFF1 (a, b) and HFF3 (c, d) cells were left uninfected (a, c) or were infected (b, d) with EV71 at an m.o.i. of 1.25. At 24 h p.i., cells were stained with Hoechst 33342 and examined under a fluorescence microscope. Arrows indicate cells with CPE. The results shown are representative of six experiments (original magnification ×200). The insert in (b) shows nuclei with a morphology typical of CPE (original magnification ×400). (e, f) HFF1 and HFF3 cells were infected with EV71 at the indicated m.o.i. At 24 (e) and 48 (f) h p.i., cell viability was determined as a percentage of the control (Con). The results are presented as means ± SD of six separate experiments. *, $P<0.05$ and **, $P<0.01$ (HFF3 vs HFF1).

medium, 100 µl DMSO was added to solubilize the formazan formed. Absorbance was measured using a microplate reader with a 570 nm test wavelength and a 690 nm reference wavelength. The $A_{570}-A_{690}$ value for each well was corrected for the blank well. The percentage viability was calculated as:

(Corrected absorbance of each experimental well/corrected absorbance of well containing uninfected cells) × 100

Microscopic examination of CPE. Chromatin condensation and the appearance of crescent-shaped nuclei were taken as the criteria of CPE (Agol *et al.*, 1998). The cell-permeable DNA dye Hoechst 33342 was added to cells at a concentration of 5 µg ml^{-1}, 15 min prior to the end of the relevant incubation time. The stained cells were examined under a fluorescence microscope.

Detection of reactive oxygen species (ROS). To visualize the formation of ROS, we examined the fluorescence of dichlorofluorescein (DCF) derived from oxidation of dihydrodichlorofluorescein (H_2DCF). Briefly, cells were infected with EV71 at an m.o.i. of 1.25. At 48 h p.i., the cells were loaded with 5 µM dichlorofluorescein diacetate (H_2DCFDA) for 20 min at 37 °C and subsequently examined under a fluorescence microscope.

ROS formation was also analysed quantitatively by flow cytometry. Briefly, cells were loaded with H_2DCFDA as described above. The loaded cells were washed twice with PBS and trypsinized for flow cytometric analysis as described previously (Royall & Ischiropoulos, 1993). The mean fluorescence intensity (MFI) of the DCF channel was quantified using CellQuest Pro software (Becton Dickinson). The percentage increase in DCF was calculated as follows:

(MFI of H_2DCFDA-loaded, infected cells) − (MFI of H_2DCFDA-loaded, uninfected cells) × 100 /(MFI of H_2DCFDA-loaded, uninfected cells)

High-performance liquid chromatographic (HPLC) analysis of glutathione (GSH) and its disulfide form (GSSG). Cells (2×10^4) were seeded into each well of a 12-well culture plate, incubated overnight and infected at the indicated m.o.i. with EV71 as described above. At 48 h p.i., the culture was rinsed once with PBS and lysed in 200 µl 1 % (w/v) metaphosphoric acid on ice. The lysate was collected and centrifuged, and the supernatant was filtered and subjected to HPLC analysis. The sample was separated by chromatography on an Inertsil ODS C18 column (5 µm, 4.6 × 250 mm; GL Sciences) and eluted at 0.8 ml min^{-1} with a mobile phase of 10 mM NaH_2PO_4 (pH 2.7)/0.3 mM octane sulfonic acid/5.1 % acetonitrile. GSH and GSSG were monitored with an ESA CoulArray multi-channel

electrochemical detector; the electrodes were set at 400, 650, 700, 800 and 850 mV.

Statistical analysis. Results are expressed as means ± SD. Data were analysed by two-way analysis of variance. A Tukey HSD test or *t*-test was used to compare the mean values of groups. *P* values of less than 0.05 were considered significant.

RESULTS

G6PD deficiency enhances EV71 replication

To investigate whether G6PD status affects the infectivity of EV71, we examined the ability of EV71 to replicate in HFF1 and HFF3 cells. As shown in Fig. 1(b, c), the number of viral progeny increased with m.o.i. of inoculum. Intriguingly, the number of progeny virions derived from infection of HFF1 cells was significantly higher than that from HFF3 cells (Fig. 1a–c).

Increased production of infectious progeny virions in G6PD-deficient cells was associated with an increase in the copy number of the viral genome. As shown in Fig. 2(i), the copy numbers of viral genomic RNA in HFF3 cells at 2, 4 and 8 h p.i. were, respectively, 1.80-, 5.40- and 238.70-fold that at 0 h p.i. In contrast, there were significantly more copies of the EV71 genome in HFF1 cells at 8 h p.i. (460.76 ± 23.55 in HFF1 vs 238.70 ± 17.64 in HFF3, $n=6$). The enhanced replication of EV71 in HFF1 cells was associated with increased expression of viral protein (Fig. 2a–h; compare panels f and h).

Increased CPE of EV71 infection is associated with G6PD deficiency

To study whether enhanced virus replication in G6PD-deficient cells correlated with CPE, we examined the CPE and viability of EV71-infected HFF1 and HFF3 cells (Fig. 3). At 24 h p.i., fibroblasts started to round up and lose contact with the substratum (data not shown). These cells displayed a nuclear morphology characteristic of CPE: the nuclei were crescent-shaped with condensed chromatin at their periphery (Fig. 3b, inset). The number of cells with these morphological changes increased as infection progressed. Interestingly, the number of cells with CPE was higher in HFF1 cells than in HFF3 cells (Fig. 3b, d). The enhanced CPE in G6PD-deficient cells was reflected by an increased loss of viability (Fig. 3e, f). The viability of the infected cells decreased with increasing m.o.i. of virus inoculum. Additionally, the viability of infected HFF1 cells was significantly lower than that of HFF3 cells at an m.o.i. above 0.6 (Fig. 3e, f). At 24 h p.i., the viability of HFF1 cells infected at an m.o.i. of 1.25 was about 21 % lower than that of HFF3 cells infected at the same m.o.i. Such discrepancy further increased as the post-infection incubation period increased to 48 h (32.44 ± 5.97 in HFF1 cells vs 55.58 ± 5.43 in HFF3 cells, $n=6$).

Increased susceptibility to EV71 infection is associated with increased oxidative stress in G6PD-deficient cells

To investigate whether a reduced ability to withstand oxidative stress in G6PD-deficient cells was associated with increased susceptibility to EV71 infection, we examined changes in the GSH : GSSG ratio in cells following infection. The GSH : GSSG ratio in uninfected HFF3 cells (32.40 ± 2.62) was higher than in HFF1 cells (20.72 ± 2.42). EV71 infection caused a decline in the GSH : GSSG ratio in an m.o.i.-dependent manner. As the m.o.i. of the inoculum increased from 0.3125 to 1.25, the GSH : GSSG ratio in HFF3 cells decreased from 23.21 ± 2.91 to 14.42 ± 1.94 (Fig. 4a). The decline was more dramatic in the case of infected HFF1 cells. At 48 h p.i., at an m.o.i. of 1.25, the GSH : GSSG ratio was decreased by over 75 %. A reduction in the GSH : GSSG ratio is indicative of increased oxidative stress in infected cells. As shown in Fig. 5, infected cells displayed elevated DCF fluorescence, with the increases being greater in HFF1 cells than in HFF3 cells.

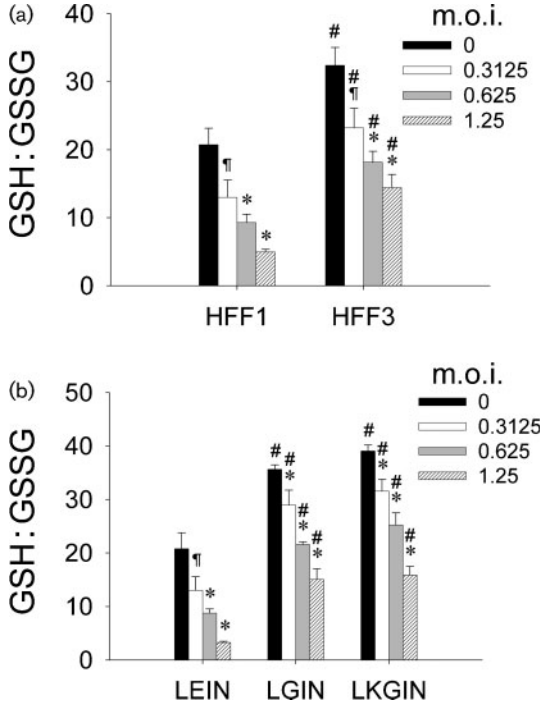

Fig. 4. Effect of EV71 infection on the intracellular GSH : GSSG ratio. (a) HFF1 and HFF3 cells were infected at an m.o.i. ranging from 0 to 1.25. At 48 h p.i., cells were harvested for analysis of GSH and GSSG content. The GSH : GSSG ratio is shown. The results are presented as means ± SD of six separate experiments. ¶, $P<0.05$ and *, $P<0.01$ (infected vs uninfected cells); #, $P<0.01$ (HFF3 vs HFF1 infected at the same m.o.i.). (b) LGIN, LKGIN and LEIN cells were analysed as in (a). The results are presented as means ± SD of six separate experiments. ¶, $P<0.05$ and *, $P<0.01$ (infected vs uninfected cells); #, $P<0.01$ (LGIN or LKGIN vs LEIN cells infected at the same m.o.i.).

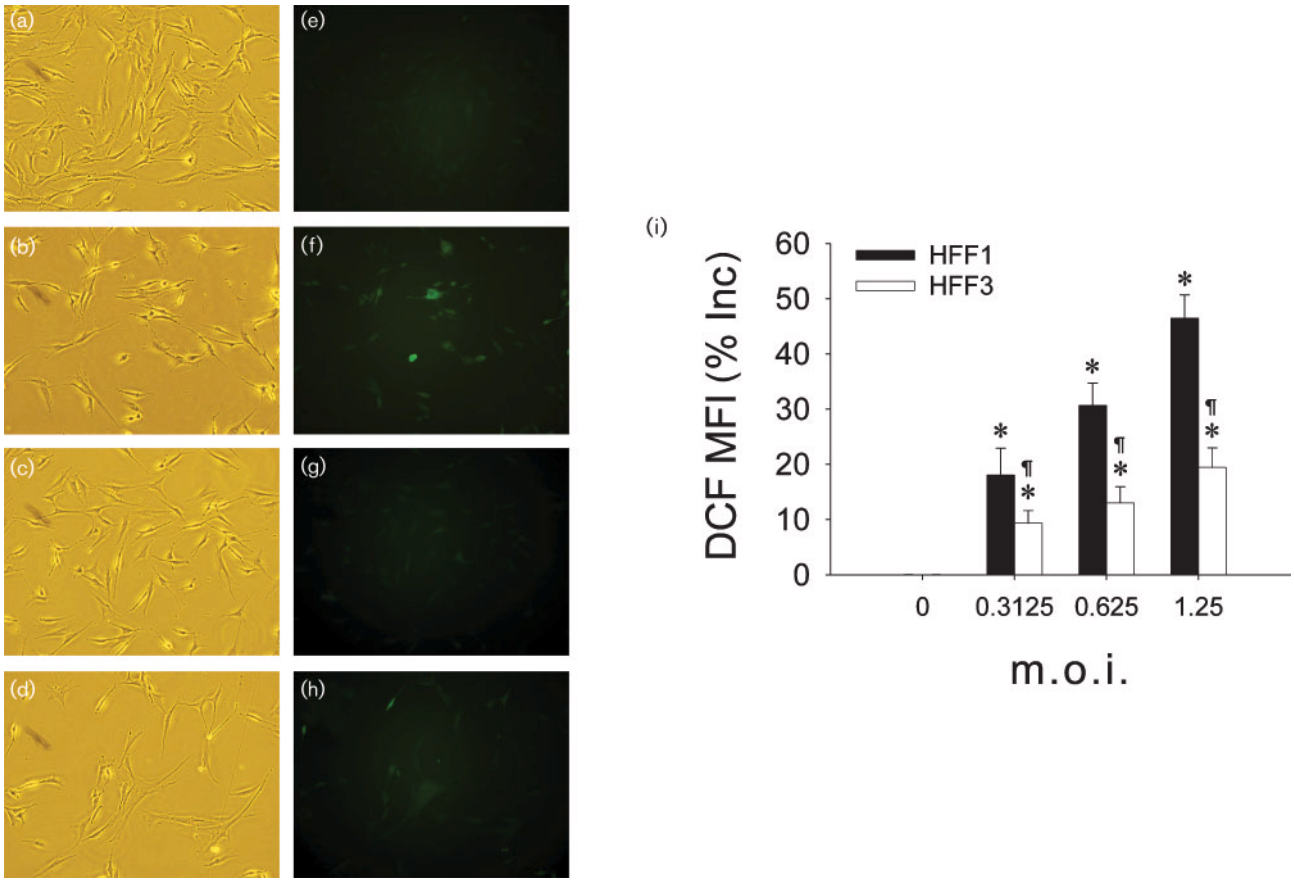

Fig. 5. EV71 infection induces oxidative stress. (a–h) HFF1 (a, b, e, f) and HFF3 (c, d, g, h) cells were left uninfected (a, c, e, g) or infected (b, d, f, h) with EV71 at an m.o.i. of 1.25. The infected cells were examined for DCF fluorescence (e–h). The corresponding phase-contrast micrographs (a–d) are also shown. Original magnification ×200. (i) HFF1 and HFF3 cells, infected at the indicated m.o.i., were harvested for flow cytometric analysis of ROS formation. The percentage increase in MFI of DCF relative to that of uninfected cells is shown. The results are presented as means ± SD of six separate experiments. *, $P<0.01$ (cells infected at the indicated m.o.i. vs uninfected cells); ¶, $P<0.05$ (HFF3 vs HFF1 cells at the same m.o.i.).

Exogenous G6PD expression increases the GSH : GSSG ratio and ameliorates cellular susceptibility to EV71 infection

To confirm that the G6PD status modulated susceptibility to EV71 infection, we infected cell lines LGIN and LKGIN, which exogenously express G6PD, with EV71 and examined the outcome of infection. LGIN and LKGIN cells have G6PD activities that are, respectively, around 18- and 19-fold that of the control cell line LEIN [2.27 ± 0.210 U (mg cell lysate)$^{-1}$ in LGIN cells and 2.40 ± 0.224 U (mg cell lysate)$^{-1}$ in LKGIN cells vs 0.125 ± 0.030 U (mg cell lysate)$^{-1}$ in LEIN cells; $n=6$]. As shown in Fig. 6, the number of progeny virions produced in LGIN and LKGIN cells was significantly reduced. At an m.o.i. of 1.25, LGIN and LKGIN cells gave rise to 53.58 and 63.21 % fewer virions than LEIN cells (Fig. 6a). When examined at 48 h p.i., the number of viral particles produced in LGIN and LKGIN cells decreased by 72.25 and 78.01 %, respectively (Fig. 6b). This was consistent with a significant reduction in the levels of progeny viral RNA in these cells (Fig. 6c). These findings clearly showed that exogenous G6PD expression reduces virus replication and the production of infectious viral progeny.

Concomitant with the decreased EV71 replication in infected LGIN and LKGIN cells, these cells displayed higher viability than infected LEIN cells; this was clearly seen at 24 h p.i. At an m.o.i. of 1.25, the viabilities of LGIN and LKGIN cells were 18.58 and 21.16 % higher than that of LEIN cells (Fig. 7a). At 48 h p.i., the differences became even more pronounced. LGIN and LKGIN cells (at an m.o.i. of 1.25) had viabilities 46.04 and 71.91 % higher than LEIN cells (Fig. 7b). In agreement with this, the number of cells with a morphology typical of CPE was lower in LGIN and LKGIN cells than in LEIN cells (data not shown).

We further tested the possibility that exogenous G6PD expression conferred resistance to EV71 infection through the potentiation of cellular antioxidant capacity. As

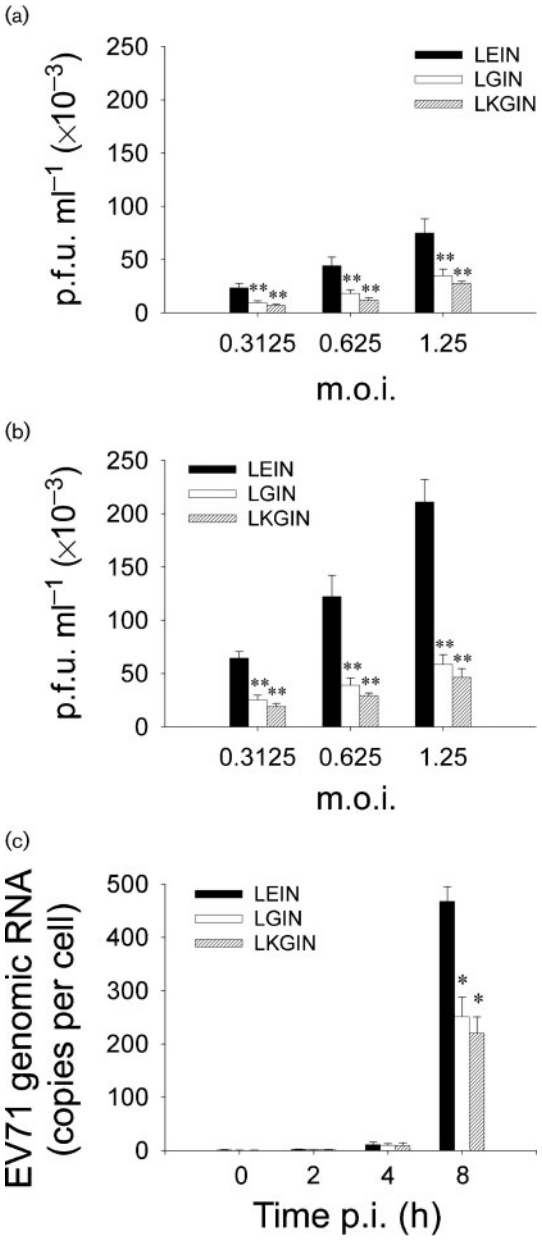

Fig. 6. Exogenous G6PD expression reduces virus replication and infectious progeny virion production. (a, b) LGIN, LKGIN or LEIN cells were infected with EV71 at the indicated m.o.i. At 24 (a) and 48 (b) h p.i., progeny viral particles were quantified. Data are expressed as p.f.u. (ml lysate)$^{-1}$. The results are presented as means ± SD of six separate experiments. **, $P<0.01$ (LGIN or LKGIN vs LEIN cells). (c) LGIN, LKGIN or LEIN cells were infected at an m.o.i. of 1.25. At the indicated times p.i., levels of EV71 genomic RNA were quantified by PCR. The results are presented as means ± SD of six separate experiments. *, $P<0.01$ (LGIN or LKGIN vs LEIN cells).

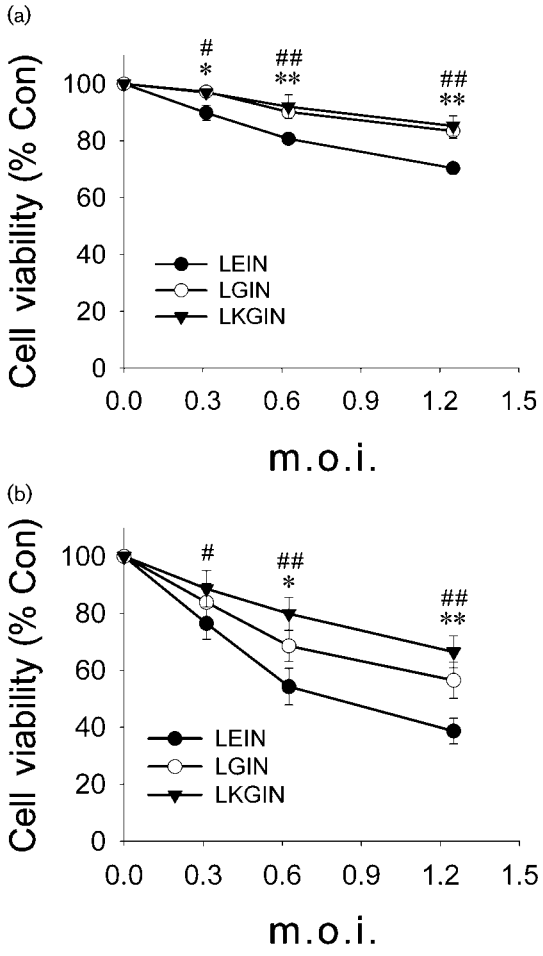

Fig. 7. Exogenous G6PD expression confers cytoprotection on EV71-infected cells. LGIN, LKGIN or LEIN cells were infected with EV71 at the indicated m.o.i. At 24 (a) and 48 (b) h p.i., cell viability was determined as a percentage of the control (Con). The results are presented as means ± SD of six separate experiments. *, $P<0.05$ and **, $P<0.01$ (LGIN vs LEIN cells); #, $P<0.05$ and ##, $P<0.01$ (LKGIN vs LEIN cells).

indicated in Fig. 4(b), the GSH : GSSG ratios of uninfected LGIN and LKGIN cells were 35.65 ± 0.85 and 39.06 ± 1.13, which were substantially higher than that of LEIN cells (20.79 ± 3.00). The decline in GSH : GSSG ratio in LGIN or LKGIN cells following EV71 infection was relatively limited. At an m.o.i. of 1.25, the GSH : GSSG ratio was reduced in LGIN and LKGIN cells by 57.82 and 59.30 %, compared with 84.34 % in LEIN cells, indicating that the higher the GSH : GSSG ratio the greater the protection against EV71 infection.

Antioxidant treatment attenuates cellular susceptibility to EV71 infection

Next, we tested whether antioxidant treatment could protect cells against EV71 infection. HFF1 and HFF3 cells were pre-treated with *N*-acetylcysteine (NAC) 1 h prior to infection with EV71 and the effects of NAC on loss of viability and the production of progeny virions were

examined. Treatment with 0.1 mM NAC restored the viabilities of infected HFF1 and HFF3 cells to 58.41 ± 5.59 and 65.38 ± 5.93 %, respectively (Fig. 8a). This cytoprotective effect was further enhanced when the NAC concentration was increased to 0.5 mM. Consistent with this, NAC significantly inhibited EV71 replication. The number of progeny virions in HFF1 and HFF3 cells was reduced by 42.50 and 48.95 %, respectively, following treatment with 0.5 mM NAC (Fig. 8b). These findings further corroborated the association between redox status and cellular susceptibility to EV71 infection.

DISCUSSION

In this study, we showed that G6PD-deficient cells are more susceptible to EV71 infection than wild-type cells. Virus replication, as indicated by levels of viral genomic RNA and the production of infectious viral progeny, was enhanced in these cells (Figs 1 and 2). It was accompanied by increased CPE and loss of viability (Fig. 3). Mechanistically, EV71 infection could by itself elicit oxidative stress (Fig. 5). The increased viral susceptibility in G6PD-deficient cells was attributed to a debilitated antioxidant defence and higher levels of oxidative stress (Fig. 4). Replenishment of G6PD increased the GSH content and offered considerable protection against infection (Figs 4, 6 and 7), reiterating the importance of G6PD as a host factor of viral infection. Mitigation of EV71 replication and cell demise by antioxidants are in line with the notion that the host cell's G6PD status affects the intracellular redox balance and determines the outcome of EV71 infection (Fig. 8).

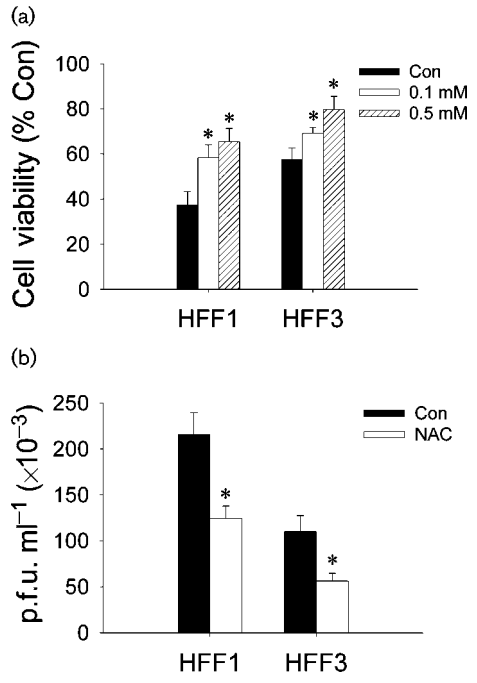

Fig. 8. Antioxidant treatment attenuates progeny virus production and cellular susceptibility to EV71 infection. (a) HFF1 and HFF3 cells were treated with the indicated concentrations of NAC 1 h prior to infection at an m.o.i. of 1.25. At 48 h p.i., the viability of infected cells was determined. The results are presented as means ± SD of six separate experiments. *, $P<0.05$ (cells treated with the indicated concentration of NAC vs untreated control). (b) In a parallel set of experiments, HFF1 and HFF3 cells were treated with 0.5 mM NAC 1 h prior to infection at an m.o.i. of 1.25. At 48 h p.i., progeny viral particles were quantified. Data are expressed as p.f.u. (ml lysate)$^{-1}$. The results are presented as means ± SD of six separate experiments. *, $P<0.05$ (cells treated with the indicated concentration of NAC vs untreated control).

A number of studies have shown that nutritional deficiencies and redox status modulate susceptibility to viral infection (Beck *et al.*, 2000, 2004). Some of these effects have been attributed to altered immune responses (Bhaskaram, 2001; Biagioli *et al.*, 1999). Using G6PD-deficient cells as a model, we demonstrated that the shift in intracellular redox milieu towards the oxidizing end enhances virus replication and CPE. Little is known about the underlying mechanism. One of the signalling pathways, the mitogen-activated protein kinase (MAPK) cascade, is redox-modulated (Fujino *et al.*, 2006; Torres & Forman, 2003) and is activated in response to EV71 infection (Wong *et al.*, 2005). It has been reported that MAPK and the stress-activated protein kinases are involved in replication of coxsackievirus B3 and encephalomyocarditis virus (Hirasawa *et al.*, 2003; Luo *et al.*, 2002). The increased ROS generation in G6PD-deficient cells may cause stronger signalling through these kinase cascades, thereby causing enhanced virus replication.

Viral infection can lead to oxidative stress (Schwarz, 1996). Levels of malondialdehyde are increased in clinical specimens from hepatitis C and AIDS patients (Gil *et al.*, 2003; Ko *et al.*, 2005; Paradis *et al.*, 1997; Turchan *et al.*, 2003). Murine infection models have indicated that increased superoxide production has been observed in pneumonia caused by influenza A virus (Oda *et al.*, 1989). Murine coxsackievirus B infection causes myocarditis and plasma glutathione depletion (Kyto *et al.*, 2004). It is conceivable that viral-induced activation of inflammatory cells partially accounts for such effects. Besides, as is the case with EV71, the virus itself can elicit ROS generation at the single-cell level. Expression of viral proteins, such as human immunodeficiency virus type 1 Tat protein and hepatitis C virus core antigen, are conducive to oxidative stress (Lachgar *et al.*, 1999; Okuda *et al.*, 2002; Toborek *et al.*, 2003). It is plausible that certain EV71 proteins may act in a similar way. Experiments are under way to test these possibilities.

Our findings suggest a model for the relationship between the redox status of the host cell and EV71. After entry into a cell, EV71 viral RNA is translated into proteins and replication ensues. These processes are sensitive to the intracellular redox environment, being more active in an

oxidizing milieu. Expression of viral protein induces ROS generation through a hitherto-unknown mechanism. This sets up a vicious cycle of ROS production and virus replication. In G6PD-deficient cells, the antioxidant capacity is limited and the intracellular environment is shifted towards the oxidizing end. The cycle is speeded up, resulting in increased CPE and virus replication, as well as oxidative stress.

Overall, our findings lend strong support to the notion that the redox status of host cells modulates the infectivity of enteroviral pathogens. It will be interesting to see whether such findings can be extrapolated to other viruses. Moreover, the finding that NAC can reduce progeny virus production raises the possibility of using antioxidants for therapeutic purposes. Antioxidant supplementation may improve the clinical situation of EV71-infected patients or be used as a preventive measure against EV71 infection.

ACKNOWLEDGEMENTS

This work was supported by grants from Chang Gung University (CMRPD160311, CMRPD160231, CMRPG330723 and CMRPD-33072), the National Science Council of Taiwan (NSC95-2320-B-182A-006, NSC96-2320-B-182A-003-MY3, NSC94-2320-B-182-036, NSC95-2320-B-182-035-MY2, NSC96-2320-B-182-015-MY3, NSC95-2320-B-182-008 and NSC95-2320-B-182-020) and the Ministry of Education of Taiwan (EMRPD160241).

REFERENCES

Agol, V. I., Belov, G. A., Bienz, K., Egger, D., Kolesnikova, M. S., Raikhlin, N. T., Romanova, L. I., Smirnova, E. A. & Tolskaya, E. A. (1998). Two types of death of poliovirus-infected cells: caspase involvement in the apoptosis but not cytopathic effect. *Virology* **252**, 343–353.

Beck, M. A., Kolbeck, P. C., Rohr, L. H., Shi, Q., Morris, V. C. & Levander, O. A. (1994a). Benign human enterovirus becomes virulent in selenium-deficient mice. *J Med Virol* **43**, 166–170.

Beck, M. A., Kolbeck, P. C., Rohr, L. H., Shi, Q., Morris, V. C. & Levander, O. A. (1994b). Vitamin E deficiency intensifies the myocardial injury of coxsackievirus B3 infection of mice. *J Nutr* **124**, 345–358.

Beck, M. A., Handy, J. & Levander, O. A. (2000). The role of oxidative stress in viral infections. *Ann N Y Acad Sci* **917**, 906–912.

Beck, M. A., Nelson, H. K., Shi, Q., Van Dael, P., Schiffrin, E. J., Blum, S., Barclay, D. & Levander, O. A. (2001). Selenium deficiency increases the pathology of an influenza virus infection. *FASEB J* **15**, 1481–1483.

Beck, M. A., Levander, O. A. & Handy, J. (2003a). Selenium deficiency and viral infection. *J Nutr* **133**, 1463S–1467S.

Beck, M. A., Williams-Toone, D. & Levander, O. A. (2003b). Coxsackievirus B3-resistant mice become susceptible in Se/vitamin E deficiency. *Free Radic Biol Med* **34**, 1263–1270.

Beck, M. A., Handy, J. & Levander, O. A. (2004). Host nutritional status: the neglected virulence factor. *Trends Microbiol* **12**, 417–423.

Beck, M. A., Shi, Q., Morris, V. C. & Levander, O. A. (2005). Benign coxsackievirus damages heart muscle in iron-loaded vitamin E-deficient mice. *Free Radic Biol Med* **38**, 112–116.

Beutler, E. (1991). Glucose-6-phosphate dehydrogenase deficiency. *N Engl J Med* **324**, 169–174.

Bhaskaram, P. (2001). Immunobiology of mild micronutrient deficiencies. *Br J Nutr* **85** (*Suppl. 2*), S75–S80.

Biagioli, M. C., Kaul, P., Singh, I. & Turner, R. B. (1999). The role of oxidative stress in rhinovirus induced elaboration of IL-8 by respiratory epithelial cells. *Free Radic Biol Med* **26**, 454–462.

Cai, J., Chen, Y., Seth, S., Furukawa, S., Compans, R. W. & Jones, D. P. (2003). Inhibition of influenza infection by glutathione. *Free Radic Biol Med* **34**, 928–936.

Cheng, M. L., Ho, H. Y., Liang, C. M., Chou, Y. H., Stern, A., Lu, F. J. & Chiu, D. T. (2000). Cellular glucose-6-phosphate dehydrogenase (G6PD) status modulates the effects of nitric oxide (NO) on human foreskin fibroblasts. *FEBS Lett* **475**, 257–262.

Cheng, A. J., Chiu, D. T., See, L. C., Liao, C. T., Chen, I. H. & Chang, J. T. (2001). Poor prognosis in nasopharyngeal cancer patients with low glucose-6-phosphate-dehydrogenase activity. *Jpn J Cancer Res* **92**, 576–581.

Cheng, M. L., Ho, H. Y., Wu, Y. H. & Chiu, D. T. (2004). Glucose-6-phosphate dehydrogenase-deficient cells show an increased propensity for oxidant-induced senescence. *Free Radic Biol Med* **36**, 580–591.

Denizot, F. & Lang, R. (1986). Rapid colorimetric assay for cell growth and survival. Modifications to the tetrazolium dye procedure giving improved sensitivity and reliability. *J Immunol Methods* **89**, 271–277.

Fujino, G., Noguchi, T., Takeda, K. & Ichijo, H. (2006). Thioredoxin and protein kinases in redox signaling. *Semin Cancer Biol* **16**, 427–435.

Gil, L., Martinez, G., Gonzalez, I., Tarinas, A., Alvarez, A., Giuliani, A., Molina, R., Tapanes, R., Perez, J. & Leon, O. S. (2003). Contribution to characterization of oxidative stress in HIV/AIDS patients. *Pharmacol Res* **47**, 217–224.

Hirasawa, K., Kim, A., Han, H. S., Han, J., Jun, H. S. & Yoon, J. W. (2003). Effect of p38 mitogen-activated protein kinase on the replication of encephalomyocarditis virus. *J Virol* **77**, 5649–5656.

Ho, M., Chen, E. R., Hsu, K. H., Twu, S. J., Chen, K. T., Tsai, S. F., Wang, J. R. & Shih, S. R. (1999). An epidemic of enterovirus 71 infection in Taiwan. Taiwan Enterovirus Epidemic Working Group. *N Engl J Med* **341**, 929–935.

Ho, H. Y., Cheng, M. L., Lu, F. J., Chou, Y. H., Stern, A., Liang, C. M. & Chiu, D. T. (2000). Enhanced oxidative stress and accelerated cellular senescence in glucose-6-phosphate dehydrogenase (G6PD)-deficient human fibroblasts. *Free Radic Biol Med* **29**, 156–169.

Ho, H. Y., Cheng, M. L. & Chiu, D. T. (2005). G6PD – an old bottle with new wine. *Chang Gung Med J* **28**, 606–612.

Ho, H. Y., Wei, T. T., Cheng, M. L. & Chiu, D. T. (2006). Green tea polyphenol epigallocatechin-3-gallate protects cells against peroxynitrite-induced cytotoxicity: modulatory effect of cellular G6PD status. *J Agric Food Chem* **54**, 1638–1645.

Ho, H. Y., Cheng, M. L., Cheng, P. F. & Chiu, D. T. (2007a). Low oxygen tension alleviates oxidative damage and delays cellular senescence in G6PD-deficient cells. *Free Radic Res* **41**, 571–579.

Ho, H. Y., Cheng, M. L. & Chiu, D. T. (2007b). Glucose-6-phosphate dehydrogenase – from oxidative stress to cellular functions and degenerative diseases. *Redox Rep* **12**, 109–118.

Huang, C. C., Liu, C. C., Chang, Y. C., Chen, C. Y., Wang, S. T. & Yeh, T. F. (1999). Neurologic complications in children with enterovirus 71 infection. *N Engl J Med* **341**, 936–942.

Ishimaru, Y., Nakano, S., Yamaoka, K. & Takami, S. (1980). Outbreaks of hand, foot, and mouth disease by enterovirus 71. High incidence of complication disorders of central nervous system. *Arch Dis Child* **55**, 583–588.

Ko, W. S., Guo, C. H., Yeh, M. S., Lin, L. Y., Hsu, G. S., Chen, P. C., Luo, M. C. & Lin, C. Y. (2005). Blood micronutrient, oxidative stress, and viral load in patients with chronic hepatitis C. *World J Gastroenterol* **11**, 4697–4702.

Kyto, V., Lapatto, R., Lakkisto, P., Saraste, A., Voipio-Pulkki, L. M., Vuorinen, T. & Pulkki, K. (2004). Glutathione depletion and cardiomyocyte apoptosis in viral myocarditis. *Eur J Clin Invest* **34**, 167–175.

Lachgar, A., Sojic, N., Arbault, S., Bruce, D., Sarasin, A., Amatore, C., Bizzini, B., Zagury, D. & Vuillaume, M. (1999). Amplification of the inflammatory cellular redox state by human immunodeficiency virus type 1-immunosuppressive Tat and gp160 proteins. *J Virol* **73**, 1447–1452.

Lin, T. Y., Chang, L. Y., Hsia, S. H., Huang, Y. C., Chiu, C. H., Hsueh, C., Shih, S. R., Liu, C. C. & Wu, M. H. (2002). The 1998 enterovirus 71 outbreak in Taiwan: pathogenesis and management. *Clin Infect Dis* **34** (*Suppl. 2*), S52–S57.

Lin, T. Y., Twu, S. J., Ho, M. S., Chang, L. Y. & Lee, C. Y. (2003). Enterovirus 71 outbreaks, Taiwan: occurrence and recognition. *Emerg Infect Dis* **9**, 291–293.

Liu, C. C., Tseng, H. W., Wang, S. M., Wang, J. R. & Su, I. J. (2000). An outbreak of enterovirus 71 infection in Taiwan, 1998: epidemiologic and clinical manifestations. *J Clin Virol* **17**, 23–30.

Luo, H., Yanagawa, B., Zhang, J., Luo, Z., Zhang, M., Esfandiarei, M., Carthy, C., Wilson, J. E., Yang, D. & McManus, B. M. (2002). Coxsackievirus B3 replication is reduced by inhibition of the extracellular signal-regulated kinase (ERK) signaling pathway. *J Virol* **76**, 3365–3373.

Luzzatto, L. & Battistuzzi, G. (1985). Glucose-6-phosphate dehydrogenase. *Adv Hum Genet* **14**, 217–329, 386–388.

McMinn, P. C. (2002). An overview of the evolution of enterovirus 71 and its clinical and public health significance. *FEMS Microbiol Rev* **26**, 91–107.

Oda, T., Akaike, T., Hamamoto, T., Suzuki, F., Hirano, T. & Maeda, H. (1989). Oxygen radicals in influenza-induced pathogenesis and treatment with pyran polymer-conjugated SOD. *Science* **244**, 974–976.

Okuda, M., Li, K., Beard, M. R., Showalter, L. A., Scholle, F., Lemon, S. M. & Weinman, S. A. (2002). Mitochondrial injury, oxidative stress, and antioxidant gene expression are induced by hepatitis C virus core protein. *Gastroenterology* **122**, 366–375.

Paradis, V., Mathurin, P., Kollinger, M., Imbert-Bismut, F., Charlotte, F., Piton, A., Opolon, P., Holstege, A., Poynard, T. & Bedossa, P. (1997). In situ detection of lipid peroxidation in chronic hepatitis C: correlation with pathological features. *J Clin Pathol* **50**, 401–406.

Racaniello, V. R. (2001). *Picornaviridae*: the viruses and their replication. In *Fields Virology*, 4th edn, pp. 685–722. Edited by B. N. Fields, D. M. Knipe, P. M. Howley & D. E. Griffin. Philadelphia: Lippincott Williams & Wilkins.

Royall, J. A. & Ischiropoulos, H. (1993). Evaluation of 2′,7′-dichlorofluorescein and dihydrorhodamine 123 as fluorescent probes for intracellular H_2O_2 in cultured endothelial cells. *Arch Biochem Biophys* **302**, 348–355.

Schmidt, N. J., Lennette, E. H. & Ho, H. H. (1974). An apparently new enterovirus isolated from patients with disease of the central nervous system. *J Infect Dis* **129**, 304–309.

Schwarz, K. B. (1996). Oxidative stress during viral infection: a review. *Free Radic Biol Med* **21**, 641–649.

Shih, S. R., Tsai, M. C., Tseng, S. N., Won, K. F., Shia, K. S., Li, W. T., Chern, J. H., Chen, G. W., Lee, C. C. & other authors (2004). Mutation in enterovirus 71 capsid protein VP1 confers resistance to the inhibitory effects of pyridyl imidazolidinone. *Antimicrob Agents Chemother* **48**, 3523–3529.

Takimoto, S., Waldman, E. A., Moreira, R. C., Kok, F., Pinheiro Fde, P., Saes, S. G., Hatch, M., de Souza, D. F., Carmona Rde, C. & other authors (1998). Enterovirus 71 infection and acute neurological disease among children in Brazil (1988–1990). *Trans R Soc Trop Med Hyg* **92**, 25–28.

Toborek, M., Lee, Y. W., Pu, H., Malecki, A., Flora, G., Garrido, R., Hennig, B., Bauer, H. C. & Nath, A. (2003). HIV-Tat protein induces oxidative and inflammatory pathways in brain endothelium. *J Neurochem* **84**, 169–179.

Torres, M. & Forman, H. J. (2003). Redox signaling and the MAP kinase pathways. *Biofactors* **17**, 287–296.

Turchan, J., Pocernich, C. B., Gairola, C., Chauhan, A., Schifitto, G., Butterfield, D. A., Buch, S., Narayan, O., Sinai, A. & other authors (2003). Oxidative stress in HIV demented patients and protection ex vivo with novel antioxidants. *Neurology* **60**, 307–314.

Wan, G. H., Tsai, S. C. & Chiu, D. T. (2002). Decreased blood activity of glucose-6-phosphate dehydrogenase associates with increased risk for diabetes mellitus. *Endocrine* **19**, 191–195.

Wong, W. R., Chen, Y. Y., Yang, S. M., Chen, Y. L. & Horng, J. T. (2005). Phosphorylation of PI3K/Akt and MAPK/ERK in an early entry step of enterovirus 71. *Life Sci* **78**, 82–90.